Published in final edited form as:
Ultrasound Med Biol. 2011 November ; 37(11): 1884–1892. doi:10.1016/j.ultrasmedbio.2011.07.012.

Bias Observed in Time-of-flight Shear Wave Speed Measurements Using Radiation Force of a Focused Ultrasound Beam

Heng Zhao[1], **Pengfei Song**[1], **Matthew W. Urban**[1], **Randall R. Kinnick**[1], **Meng Yin**[2], **James F. Greenleaf**[1], and **Shigao Chen**[1]

[1] Department of Physiology and Biomedical Engineering, Mayo Clinic College of Medicine, Rochester, MN

[2] Department of Radiology, Mayo Clinic College of Medicine, Rochester, MN

Abstract

Measurement of shear wave propagation speed has important clinical applications because it is related to tissue stiffness and health state. Shear waves can be generated in tissues by the radiation force of a focused ultrasound beam (push beam). Shear wave speed can be measured by tracking its propagation laterally from the push beam focus using the time-of-flight principle. This study shows that shear wave speed measurements with such methods can be transducer, depth, and lateral tracking range dependent. Three homogeneous phantoms with different stiffness were studied using curvilinear and linear array transducer. Shear wave speed measurements were made at different depths, using different aperture sizes for push, and at different lateral distance ranges from the push beam. The curvilinear transducer shows a relatively large measurement bias that is depth dependent. The possible causes of the bias and options for correction are discussed. These bias errors must be taken into account to provide accurate and precise time-of-flight shear wave speed measurements for clinical use.

Keywords

Shear wave speed; Liver fibrosis; Bias; ARFI

INTRODUCTION

Mechanical properties of tissues such as shear modulus (elasticity) are related to the state of tissue health (Sarvazyan et al. 1998). Therefore, non-invasive methods for measuring tissue elasticity have important clinical applications. Assuming isotropy, incompressibility, and linearity, the shear modulus μ of a soft tissue is related to its shear wave propagation speed c_s by Eq. (1)

Corresponding Author: Shigao Chen Address: 200 First Street, S.W., Rochester, MN 55905 U.S.A. Phone: 507-284-8252 Fax: 507-266-0361 chen.shigao@mayo.edu.

$$\mu=\rho c_s^2, \quad (1)$$

where ρ is density which can be assumed to be 1000 kg/m^3 for all soft tissues (Yamakoshi et al. 1990). Equation (1) neglects tissue viscosity and frequency effects, but generally is considered valid when the frequency of the shear wave is low and narrowband. Therefore, measurements of shear wave propagation speed can be used to estimate tissue elasticity for that bandwidth present in the shear wave.

Acoustic radiation force from a focused ultrasound beam can be used to generate shear waves within tissues. If a single focused ultrasound beam is used for pushing, it is commonly assumed that the shear waves generated by the ultrasound radiation force at the focal region propagate within the transducer imaging plane in a direction perpendicular to the ultrasound beam axis (Parker et al. 2011). Therefore, tissue motion at several lateral positions along the shear wave propagation path at the push beam focal depth can be measured using pulse-echo ultrasound to calculate shear wave propagation speed based on time-of-flight principle. This approach was first proposed in Shear Wave Elasticity Imaging (SWEI) and later used by several groups with various modifications to measure tissue elasticity (Chen et al. 2009; Deffieux et al. 2009; Palmeri et al. 2008; Sarvazyan et al. 1998). Among these methods, Supersonic Shear Imaging (SSI) and Acoustic Radiation Force Impulse imaging (ARFI) have been implemented on commercial ultrasound scanners and used for human studies (D'Onofrio et al. 2010; Deffieux et al. 2009; Muller et al. 2009; Palmeri et al. 2008; Tanter et al. 2008).

The purpose of this study is to evaluate if shear wave speed measured by radiation force of a focused ultrasound beam and time-of-flight method is affected by measurement conditions such as the transducer used and measurement location. A systematic phantom study reveals that measured shear wave speeds can be transducer dependent, depth dependent, and lateral tracking range dependent. Measurement bias is large enough to potentially change diagnosis, for example, in liver fibrosis staging. Findings in this study have important implications on clinical applications of shear wave speed measurements using ultrasound radiation force produced by a focused ultrasound beam.

METHOD

Phantom study design

The phantom study was designed to determine whether shear wave speed measurements are depth dependent, transducer dependent, or lateral tracking range dependent, even in homogenous phantoms. Three homogenous elasticity phantoms (custom made by CIRS, Inc. Norfolk, VA) with different elasticity values were used in this study. Each phantom had a dimension of $10 \times 10 \times 8$ cm^3 (width, depth, height). Shear wave speed measurements were made using a curvilinear transducer C4-2 and a linear array transducer L7-4 (Philips Healthcare, Andover, MA) in each phantom. The focal point of push beam in this study was positioned at different depths without any steering. For the C4-2 transducer, measurements were made with the transducer focusing at depths of 30, 40, 50, 60, and 70 mm away from the transducer surface. For the L7-4 transducer, measurements were made at focal depths of 20, 25, 30, 35, and 40 mm. A shallower depth range was chosen for the L7-4 to reflect typical measurement depths expected for this higher frequency transducer. Three different transmit aperture sizes (32, 64, and 96 elements) were used to produce shear waves at each focal depth. At each of the setup combinations mentioned above, 5 repeated measurements were made by positioning the transducer at 5 different locations on the phantom surface. The locations were selected randomly near the center of each phantom to avoid potential

influence of the boundaries for measurements (no reflection of shear waves from boundaries were observed in this study using flash imaging described in the next paragraph). Therefore, we have a total of 450 shear wave measurements in this study (3 phantoms by 2 transducers by 5 depths by 3 aperture sizes by 5 repetitions). To determine whether shear wave speed measurements depend on lateral range, shear wave speed was also calculated from two different lateral distance ranges from the push beam: 0~7.7 mm and 7.7~15.4 mm for the C4-2 and 0~9.2 mm and 9.2~18.5 mm for the L7-4. Therefore, a total of 450×2 = 900 shear wave speed estimates are reported in this study.

Shear wave speed measurement

A Verasonics ultrasound system (Verasonics Inc., Redmond, WA) was used in this study to make shear wave speed measurements. For the C4-2 transducer, the push beam for shear wave generation had a center frequency of 3 MHz and duration of 331 μs. For the L7-4 transducer, the push beam for shear wave generation had a center frequency of 5 MHz and duration of 128 μs. The push pulse duration was selected such that sufficient shear wave motion (at least several microns) could be produced without exceeding the capacity of the transmission circuit of the Verasonics system. Propagation of shear waves was monitored for 20 ms at a frequency of 4 kHz using "flash" imaging. In flash imaging mode, the Verasonics ultrasound system transmitted an unfocused ultrasound pulse (a "plane wave" compared to a traditional focused ultrasound "beam") into the imaged medium and used parallel channel processing to generate one complete two-dimensional (2D) ultrasound image from one transmission (Bercoff et al. 2004a). The center frequencies used for imaging pulses were 3 MHz for the C4-2 and 5 MHz for the L7-4. Therefore, shear wave motion can be detected within a 2D region (with a pixel resolution of one ultrasound wavelength which was 0.51 mm for the C-2 and 0.31 mm for the L7-4) at high pulse repetition frequency (PRF) which was 4 kHz in this study. Shear wave displacement was calculated from in-phase/quadrature (IQ) data using one-dimensional (1D) autocorrelation method (Kasai et al. 1985). Shear wave displacement at the focal depth of the push beam was averaged over 10 wavelengths (corresponding to an axial range of 5 mm for C4-2 and 3 mm for the L7-4) along the beam axis to improve signal-to-noise ratio (SNR). Shear wave speed (group velocity) was then estimated from the arrival time (using time-to-peak) of the shear wave at different lateral distance from the push beam center through linear regression (Palmeri et al. 2008).

Independent measurement of phantom elasticity

Shear wave speed in all three elasticity phantoms used in this study were measured by Magnetic Resonance Elastography (MRE) (Muthupillai et al. 1995) and 1D Transient Elastography (TE) (Sandrin et al. 2002) for independent comparison. MRE measurements were made using a 3.0T whole-body magnetic resonance imaging system (GE Medical System, Milwaukee, WI, USA) at a shear wave frequency of 100 Hz. A multi-slice spin echo based echo planar MRE sequence with four phase offsets was used to collect three-dimensional (3D) shear wave data with three orthogonal motion sensitizing directions. After curl filtering to remove the undesired bulk motion, 3D local frequency estimation (LFE) inversion was performed to calculate shear wave speed (Manduca et al. 2001). Shear wave speeds measured at three orthogonal directions were averaged at each voxel to give a single estimate of speed at each spatial location.

For the 1D Transient Elastography (TE) experiments, a 6.4 mm diameter, weakly focused (nominal focal range: 1~7 cm), 7.5 MHz single-element transducer (ECHO Ultrasound, Lewistown, PA) was attached to a mechanical vibrator (V203, Ling Dynamic Systems Limited, Hertfordshire, UK), so that the transducer can vibrate on the phantom surface during pulse-echo motion detection. A single-cycle 100 Hz sinusoidal pulse was used to

drive the vibrator for shear wave generation through the transducer into the phantom under test. Transducer motion was removed from shear wave displacement demodulated from radiofrequency (RF) ultrasound echo signals (Sandrin et al. 2002). Shear wave propagation from 5 mm to 35 mm in depth away from the transducer surface was used to calculate shear wave speed. Measurements were repeated five times at different locations across the surface of each elasticity phantom.

Measurement of transducer intensity field

To evaluate the influence on shear wave speed measurements due to the force field of the push beam used for shear wave generation, the pressure field of the push beam was measured using a calibrated needle hydrophone (HGL0200 by ONDA Corporation, Sunnyvale, CA), and the intensity was derived by using the equation $I = p^2/\rho c$, where p is the pressure and ρ and c are the density and sound speed of the medium, respectively. Two-dimensional scans were performed with a spatial resolution of 0.5 mm in the mid-elevational plane (x-z plane) and mid-lateral plane (y-z) of the C4-2 and L7-4 transducers, where x, y, z represent the lateral, elevational, and axial directions of the ultrasound transducer, respectively. Measurements were performed in a water tank where the transducer repeatedly transmitted the push pulse while the hydrophone was translated by step motors to scan the pressure field. To protect the Verasonics system and tested transducers, each transmitted pulse consisted of 32 cycles of ultrasound (10.7 μs for C4-2 and 6.4 μs for L7-4). No appreciable difference of pressure field was found by increasing the pulse durations to those used in shear wave speed measurements. Scans were obtained for the C4-2 focusing at 30 and 50 mm, and for the L7-4 focusing at 20 and 30 mm from the transducer surface. All measurements were made with 64 transducer elements used for push beam transmission.

Statistical analysis

Paired t-test was used to evaluate for each transducer if there was a significant difference between shear wave speed measurements made at different depths, different lateral ranges from the push beam, or using different aperture sizes for push beam transmission. Because the shear wave speeds of 5 repeated measurements made at each setup combination had small variation (standard deviation around 0.01 m/s), the mean value was treated as a single sample for that combination in the paired t-test. To test the difference between two lateral ranges using the C4-2 transducer, we paired samples from all focus depths, all aperture sizes, and all phantoms. A similar pairing strategy was used to test the difference between focus depths, and the difference between aperture sizes. The same analysis was repeated for the L7-4. A p-value less than 0.05 indicated that the measurements were statistically significantly different.

RESULTS

Shear wave speeds measured by MRE and 1D TE

Figure 1 shows the shear wave speed measured by MRE in 3 phantoms. Within each phantom, the mean and standard deviation of the shear wave speed was calculated from a 6 × 6 cm^2 region at the center of the phantom for each depth. Results at the top 1 cm and bottom 1 cm were not given here because these may be affected by boundary effects. Small variation of shear wave speed measured along depth may be due to resonance of the phantom. The mean and standard deviations of shear wave speed mean values along all depths shown in Fig. 1 are 1.24 ± 0.01 m/s, 1.47 ± 0.02 m/s, and 1.80 ± 0.02 m/s for phantoms 1, 2, and 3, respectively. These results suggest that all phantoms are indeed spatially homogenous in terms of shear wave speed. Results obtained from 1D TE are very close to those of the MRE tests: 1.23 ± 0.02 m/s, 1.48 ± 0.03 m/s, and 1.89 ± 0.07 m/s for phantom 1, 2, and 3, respectively. These results are summarized in Table 1. No significant

difference was found by Student's t-test between MRE and 1D TE results for phantoms 1 and 2 ($p > 0.05$). Phantom 3 showed a significant difference ($p < 0.01$).

Shear wave speed measured using ultrasound radiation force

Shear wave speeds measured by the C4-2 transducer at different depths using different transmit aperture sizes are shown in Fig. 2. Shear wave speeds were measured using a lateral range of 0~15.4 mm from the push beam focus. Different vertical scales are chosen for each phantom in order to better show the differences in data. Shear wave speeds measured at different depths are significantly different ($p < 0.01$ for any two different depths). There are no significant differences using different push aperture sizes for measurements ($p > 0.05$).

Shear wave speeds measured by the L7-4 transducer at different depths and with different transmit aperture size are shown in Fig. 3. Shear wave speeds were measured using a lateral range of 0~18.48 mm from the push beam focus. Shear wave speeds measured with different aperture sizes are significantly different ($p < 0.01$ for any two different aperture sizes). Results are mixed for different focal depths: some are significant and some are not. The *p*-values of paired t-test for depth are shown in Table 2.

Shear wave speeds measured by the C4-2 transducer using two different lateral ranges (0~7.7 mm and 7.7~15.4 mm) from the push beam are shown in Fig. 4. Measurement differences due to different lateral ranges are statistically significant ($p < 0.01$). Shear wave speeds measured by the L7-4 transducer using two different lateral ranges (0~9.24 mm and 9.24~18.48 mm) from the push beam are shown in Fig. 5. Measurement differences due to different lateral ranges are also statistically significant ($p < 0.01$) for this transducer.

Transducer intensity field measurements

The measured intensity fields of the C4-2 focused at 30 and 50 mm in depth are shown in Fig. 6. 2D images of the intensity field are presented here for the mid-elevational plane (*x*-*z* plane) and mid-lateral plane (*y*-*z* plane). When the transducer is focused at 30 mm, focusing in the lateral direction is good. However, there are two split peaks in the elevational direction of the transducer, which can be seen clearly in the *y*-*z* plane scan. Computer simulation with Field II (Jensen and Svendsen 1992) confirms the presence of the split peaks but these simulation results are not shown here for the sake of succinctness. The C4-2 has a fixed elevational focus at about 70 mm in depth. Focusing the C4-2 too close to the transducer surface may cause undesired features in the elevational direction such as the split peaks at 30 mm focal depth. Note that these measurements were made with relatively long transmission tonebursts required in SWEI measurements. Focusing in elevational direction is better for short transmission pulses used for imaging. The split peaks produce shear waves that travel out-of-plane to the shear wave detection plane (*x*-*z* plane in Fig. 6). Implications of split peaks in shear wave speed measurements will be discussed in the next section. Referring to Fig. 6(b), focusing is better in both lateral and elevational direction when the C4-2 is focused at 50 mm in depth.

The measured intensity fields of the L7-4 focusing at 20 and 30 mm in depth are shown in Fig. 7. Two-dimensional images of the intensity field are presented here for the mid-elevational plane (x-z plane) and mid-lateral plane (*y*-*z* plane). Focusing is good in both lateral and elevational directions. The L7-4 has a fixed elevational focus at about 25 mm in depth.

DISCUSSION

Data in this study show that shear wave speeds produced with radiation force of a focused ultrasound beam and time-of-flight can be transducer dependent, depth dependent, and

lateral range dependent. It was found that shear wave speed measured by the C4-2 transducer increased when measurements were made closer to the transducer surface. This finding is consistent with results reported by D'Onofrio, *et al*. (D'Onofrio et al. 2010), where ARFI with a different curvilinear transducer was used to measure liver shear wave speed in 20 healthy volunteers. They reported that the mean shear wave speed was 1.56 m/s in deep portion versus 1.90 m/s in shallow portion of the right lobe. Another study in healthy volunteers reported similar findings (Kaminuma et al. 2011). However, this difference was thought to be due to inherent liver "stiffness" variation or compression from transducer or cardiovascular system. Results from this study suggest that this difference might instead be due to depth dependent measurement bias. Referring to Eq. (1), a small bias in shear wave speed can result in a bigger bias in elasticity because the shear modulus is proportional to square of shear wave speed. For example, the shear wave speed measured by the C4-2 in phantom 2 was about 1.7 m/s at 30 mm depth and 1.5 m/s at 70 mm depth, giving values of μ of 2.3 kPa and 2.9 kPa from Eq. (1). Using the cutoff values from a MRE study with 133 liver biopsy patients (Huwart et al. 2008), this can lead to a difference between F0 (no fibrosis) and F ≥ 2 (stage 2 fibrosis or higher). Therefore, bias occurring in clinically relevant measurement conditions can be large enough to change diagnosis results and clinical decision making.

One possible cause of depth dependent bias in C4-2 measurements is the undesired intensity field of the push beam. The force field F, which is proportional to the intensity field where the force per unit volume, can be written as $F = 2\alpha I/c$ where α and c are the ultrasound attenuation and sound speed of the medium. According to Fig. 6(a), the push beam generating the radiation force has two peaks with equal distance from the mid-elevational plane. Figure 8 is a simplified illustration of the force field in the transducer focal plane. The broken line rectangular box represents the transducer with its ultrasound beam directing into plane of this figure. The two peaks are represented by Source 1 and Source 2 which are confined within this figure but have longer axial extension out of the figure plane. Shear wave speed is estimated from the arrival time along the mid-elevational line represented by the solid horizontal line in Fig. 8. At time t_1 and t_2 , the shear wave travels distance a and b to intersect with the horizontal line where shear wave detections are made. If the real shear wave speed of the medium is c_0 , then $a = c_0 t_1$ and $b = c_0 t_2$ (the shear waves from source 2 are not shown in Fig. 8 for clarity of presentation). However, the apparent shear wave speed by measuring the arrival time along the mid-elevational line is:

$$\tilde{c}=\frac{d}{t_2-t_1}=\frac{\sqrt{a^2+b^2-2ab\cos\theta}}{t_2-t_1}\geq\frac{\sqrt{a^2+b^2-2ab}}{t_2-t_1}=\frac{b-a}{t_2-t_1}=\frac{c_0t_2-c_0t_1}{t_2-t_1}=c_0 \quad (2)$$

Therefore, the measured shear wave speed is always greater than the true wave speed. When the C4-2 is focused deeper, Sources 1 and 2 will be closer to the mid-elevational plane and the bias will be smaller. Figure 6(b) shows a single peak in elevational direction when the transducer is focused at 50 mm in depth. However, a relatively wide beam width in the elevational direction can still generate significant out-of-plane shear waves that introduce bias (though smaller) to speed measurements.

The bias in shear wave speed measurement also depends on the lateral range used for speed measurement: bias is smaller when the measurement range d in Fig. 8 is farther away from the sources (smaller θ and therefore smaller $\tilde{c}$). This is consistent with the results in Fig. 4.

Figure 6 also shows non-zero intensity before and beyond the transducer focus, which has an "X" shape in the x-z plane. Therefore, additional shear waves generated from these non-focal regions can propagate to the focal plane and interfere with the shear wave coming from

the focal zone. The apparent speed of these additional shear waves will be different from the true shear wave speed if measured along the lateral direction at the focal plane, because the lateral measurement direction is not parallel with the propagation direction of these additional shear waves. Different aperture sizes (32, 64, and 96 elements) for push beam transmission used in this study will change the angle of the "X" shape. Figure 2 indicates that different aperture size does not change shear wave speed measured by the C4-2 significantly at any given depth. This seems to suggest that for the C4-2, bias in shear wave speed measurement may be influenced more by the push beam shape in the *y*-*z* plane than that in the *x*-*z* plane.

Focusing of the L7-4 is good in both lateral and elevational direction at a focal depth as small as 20 mm, and the shear wave speed measured with the L7-4 shows little dependence with focal depth. Compared to the C4-2, the L7-4 shows more obvious change with different aperture size. This is not surprising because wider aperture size should not change the X beam shape too much for the C4-2 (outer elements contribute little to the focused beam because they are oriented away from the focus due to the curvature of the transducer). Similar to the C4-2, the L7-4 consistently shows higher shear wave speed at lateral range close to the push beam.

The potential sources of error discussed above are associated with time-of-flight based estimators relying on *a priori* information about the shear wave propagation direction from a focused beam. More advanced inversion algorithms that do not make such assumptions will not be affected by this source of error. However, it is not uncommon for ultrasound based direct inversion methods (Bercoff et al. 2004a) to assume negligible out-of-plane propagations, the validity of which may require further investigations.

Other than the push beam shape, dispersion is another possible reason for the measurement biases observed in this study. Equation (1) assumes a pure elastic medium. For viscoelastic materials, shear wave speed is dispersive and frequency dependent (Chen et al. 2009). Therefore, if the frequency band of the shear wave changes with focus depth, aperture size, or lateral range, the measured shear wave speed can also change due to dispersion caused by material viscosity. Figure 9 shows the power spectra of shear waves (recorded 5 mm away from the push beam) generated by the C4-2 with different focal depths in phantom 1. The spectra are similar to each other. These results seem to suggest that viscous dispersion is not the main cause of the depth dependent bias for C4-2. Note that these experiments were performed in phantoms made with Zerdine®, which has low viscosity (Havre et al. 2008). Tissue has higher viscosity and therefore the impact of dispersion effects requires further investigations.

There are a couple of possible options to correct for the shear wave speed measurement bias. One can use homogenous phantoms with known viscoelasticity to calibrate measurements made at different depth and steered angle. The transducer, its aperture size used for the push beam, and the lateral range used in shear wave speed measurement are usually fixed for a given clinical application. The calibration would only need to cover the viscoelastic range and measurement locations expected in a particular clinical application. For a curvilinear array, the active aperture can be translated along the curved surface of the transducer to produce push beams at different angles without real "steering". Therefore, the correction factor probably will be insensitive to "steering angle" in this case because the push beam shape and frequency content of the shear wave should not change significantly for different push beam angles. The shear wave speed was measured in phantom 2 using 5 different push beam angles (0°, 4.7°, 9.5°, 14.2°, and 18.9°) when focusing at 30 mm with the C4-2. Variation of shear wave speed measurements among these 5 angles were less than 0.06 m/s (data not shown). A calibration table can be generated and used to correct for measurements

in real tissues. Interpolation may be needed to increase the "resolution" of such a calibration table.

Another correction option is through simulation. The intensity field of the push beam can be calculated and used to compute the force field of the push beam. Shear waves generated by the push beam can be simulated with Finite Element Method (Palmeri et al. 2005) or Green's function (Bercoff et al. 2004b). Measurement bias along the lateral direction at the focal depth can then be estimated from these simulations and used to correct real tissue measurements. A correction table similar to the phantom calibration approach can be generated by the simulation method. The 3D beam shape for pulse-echo detection can also introduce averaging to shear wave motion detection (Palmeri et al. 2006) and therefore should also be accounted for in the simulation correction approach.

This study has some limitations. First, the possible reasons for these observed biases in shear wave speed measurement are hypothetical and not confirmed. This study is intended as a "case report" to alert investigators in this field of a potential problem in these measurements. Further investigations are required to understand and confirm the mechanism causing this phenomenon. The simulation approach outlined above may provide valuable insights into this investigation. Second, the MRE and 1D TE utilized different excitation sources, shear wave frequencies, reconstruction algorithms, and regions of interest that introduce additional unknowns for the comparison with shear wave speed measured by time-of-flight with radiation force, making them not ideal control experiments. Third, shear wave detection in this study used flash imaging, which is different from the typical focused "beam" detection in other methods such as ARFI. Therefore, results in this study may be different from other methods where beam detection is used. SNR of echoes from flash imaging may not be as high as that from the focused beam detection schemes. Displacement tracking errors associated with scatterer shearing within the tracking point spread function (Palmeri et al. 2006) is also different for flash imaging. However, shear waves detected by flash imaging matched simulation by Green's function very well in viscoelastic phantom studies, suggesting that flash imaging can provide reliable tracking of shear waves (Bercoff et al. 2004b).

CONCLUSION

It is shown with a systematic phantom study that time-of-flight shear wave speed measurements using radiation force produced by a focused ultrasound beam can be dependent on transducer geometry, focusing depth, and lateral tracking range used. Measurement bias can be large in terms of clinical relevance and therefore require careful monitoring or correction.

Acknowledgments

This work was supported by NIH grants DK082408, EB02640, and EB001981. The authors thank Dr. Richard Ehman for his support of MRE measurements on phantoms used in this study.

REFERENCES

Bercoff J, Tanter M, Fink M. Supersonic shear imaging: A new technique for soft tissue elasticity mapping. IEEE Transactions on Ultrasonics Ferroelectrics and Frequency Control. 2004a; 51:396–409.

Bercoff J, Tanter M, Muller M, Fink M. The role of viscosity in the impulse diffraction field of elastic waves induced by the acoustic radiation force. IEEE Transactions on Ultrasonics Ferroelectrics and Frequency Control. 2004b; 51:1523–36.

Chen SG, Urban MW, Pislaru C, Kinnick R, Zheng Y, Yao AP, Greenleaf JF. Shearwave Dispersion Ultrasound Vibrometry (SDUV) for Measuring Tissue Elasticity and Viscosity. IEEE Transactions on Ultrasonics Ferroelectrics and Frequency Control. 2009; 56:55–62.

D'Onofrio M, Gallotti A, Mucelli RP. Tissue quantification with acoustic radiation force impulse imaging: Measurement repeatability and normal values in the healthy liver. AJR Am J Roentgenol. 2010; 195:132–6. [PubMed: 20566806]

Deffieux T, Montaldo G, Tanter M, Fink M. Shear wave spectroscopy for in vivo quantification of human soft tissues visco-elasticity. IEEE Trans Med Imaging. 2009; 28:313–22. [PubMed: 19244004]

Havre RF, Elde E, Gilja OH, Odegaard S, Eide GE, Matre K, Nesje LB. Freehand real-time elastography: impact of scanning parameters on image quality and in vitro intra- and interobserver validations. Ultrasound Med Biol. 2008; 34:1638–50. [PubMed: 18524458]

Huwart L, Sempoux C, Vicaut E, Salameh N, Annet L, Danse E, Peeters F, ter Beek LC, Rahier J, Sinkus R, Horsmans Y, Van Beers BE. Magnetic resonance elastography for the noninvasive staging of liver fibrosis. Gastroenterology. 2008; 135:32–40. [PubMed: 18471441]

Jensen JA, Svendsen NB. Calculation of pressure fields from arbitrarily shaped, apodized, and excited ultrasound transducers. IEEE Trans Ultrason Ferroelectr Freq Control. 1992; 39:262–7. [PubMed: 18263145]

Kaminuma C, Tsushima Y, Matsumoto N, Kurabayashi T, Taketomi-Takahashi A, Endo K. Reliable measurement procedure of virtual touch tissue quantification with acoustic radiation force impulse imaging. J Ultrasound Med. 2011; 30:745–51. [PubMed: 21632988]

Kasai C, Namekawa K, Koyano A, Omoto R. Real-time two-dimensional blood flow imaging using an autocorrelation technique. IEEE Transactions on Sonics and Ultrasonics. 1985; Su-32:458–64.

Manduca A, Oliphant TE, Dresner MA, Mahowald JL, Kruse SA, Amromin E, Felmlee JP, Greenleaf JF, Ehman RL. Magnetic resonance elastography: non-invasive mapping of tissue elasticity. Med Image Anal. 2001; 5:237–54. [PubMed: 11731304]

Muller M, Gennisson JL, Deffieux T, Tanter M, Fink M. Quantitative Viscoelasticity Mapping of Human Liver Using Supersonic Shear Imaging: Preliminary in Vivo Feasability Study. Ultrasound in Medicine and Biology. 2009; 35:219–29. [PubMed: 19081665]

Muthupillai R, Lomas DJ, Rossman PJ, Greenleaf JF, Manduca A, Ehman RL. Magnetic-Resonance Elastography by Direct Visualization of Propagating Acoustic Strain Waves. Science. 1995; 269:1854–57. [PubMed: 7569924]

Palmeri ML, McAleavey SA, Trahey GE, Nightingale KR. Ultrasonic tracking of acoustic radiation force-induced displacements in homogeneous media. IEEE Trans Ultrason Ferroelectr Freq Control. 2006; 53:1300–13. [PubMed: 16889337]

Palmeri ML, Sharma AC, Bouchard RR, Nightingale RW, Nightingale KR. A finite-element method model of soft tissue response to impulsive acoustic radiation force. IEEE Trans Ultrason Ferroelectr Freq Control. 2005; 52:1699–712. [PubMed: 16382621]

Palmeri ML, Wang MH, Dahl JJ, Frinkley KD, Nightingale KR. Quantifying hepatic shear modulus in vivo using acoustic radiation force. Ultrasound Med Biol. 2008; 34:546–58. [PubMed: 18222031]

Parker KJ, Doyley MM, Rubens DJ. Imaging the elastic properties of tissue: the 20 year perspective. Physics in Medicine and Biology. 2011; 56:R1–R29. [PubMed: 21119234]

Sandrin L, Tanter M, Gennisson JL, Catheline S, Fink M. Shear elasticity probe for soft tissues with 1-D transient elastography. Ieee Transactions on Ultrasonics Ferroelectrics and Frequency Control. 2002; 49:436–46.

Sarvazyan AP, Rudenko OV, Swanson SD, Fowlkes JB, Emelianov SY. Shear wave elasticity imaging: A new ultrasonic technology of medical diagnostics. Ultrasound in Medicine and Biology. 1998; 24:1419–35. [PubMed: 10385964]

Tanter M, Bercoff J, Athanasiou A, Deffieux T, Gennisson JL, Montaldo G, Muller M, Tardivon A, Fink M. Quantitative assessment of breast lesion viscoelasticity: Initial clinical results using supersonic shear imaging. Ultrasound in Medicine and Biology. 2008; 34:1373–86. [PubMed: 18395961]

Yamakoshi Y, Sato J, Sato T. Ultrasonic imaging of internal vibration of soft tissue under forced vibration. IEEE Trans Ultrason Ferroelectr Freq Control. 1990; 37:45–53. [PubMed: 18285015]

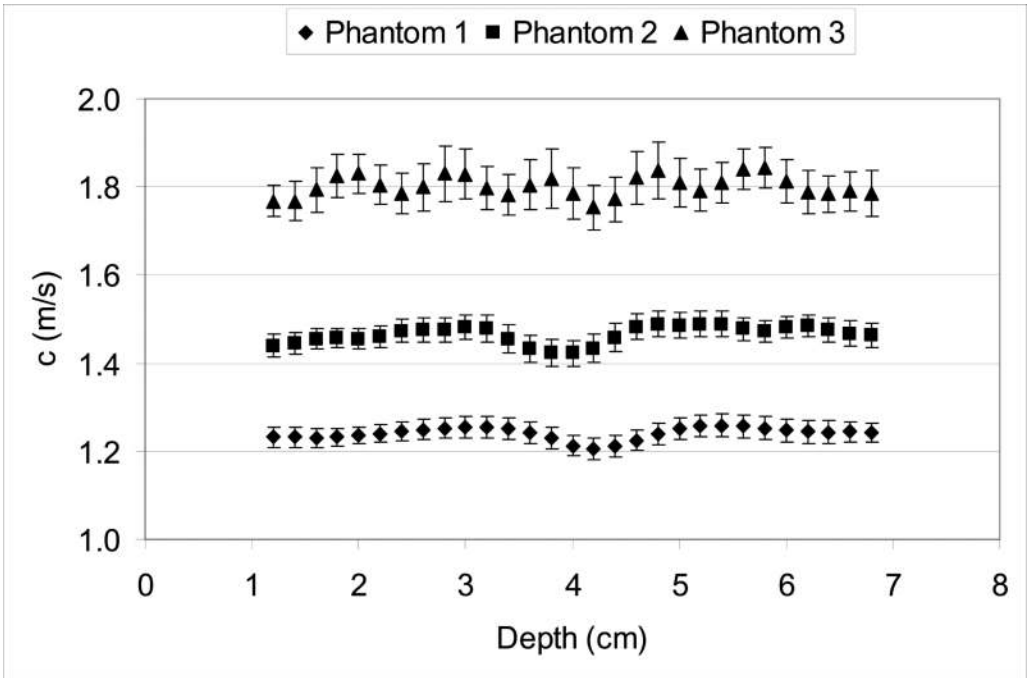

Fig. 1.
Shear wave speed measured by MRE in 3 phantoms.

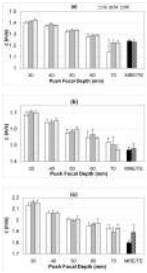

Fig. 2.
Shear wave speeds measured by C4-2 (elevational focus: 70 mm) in phantom 1 (a), phantom 2 (b), and phantom 3 (c). At each measurement depth, 3 different aperture sizes (32, 64, and 96 elements) were used for push beam transmission. Results from MRE and 1D TE are also displayed for comparison.

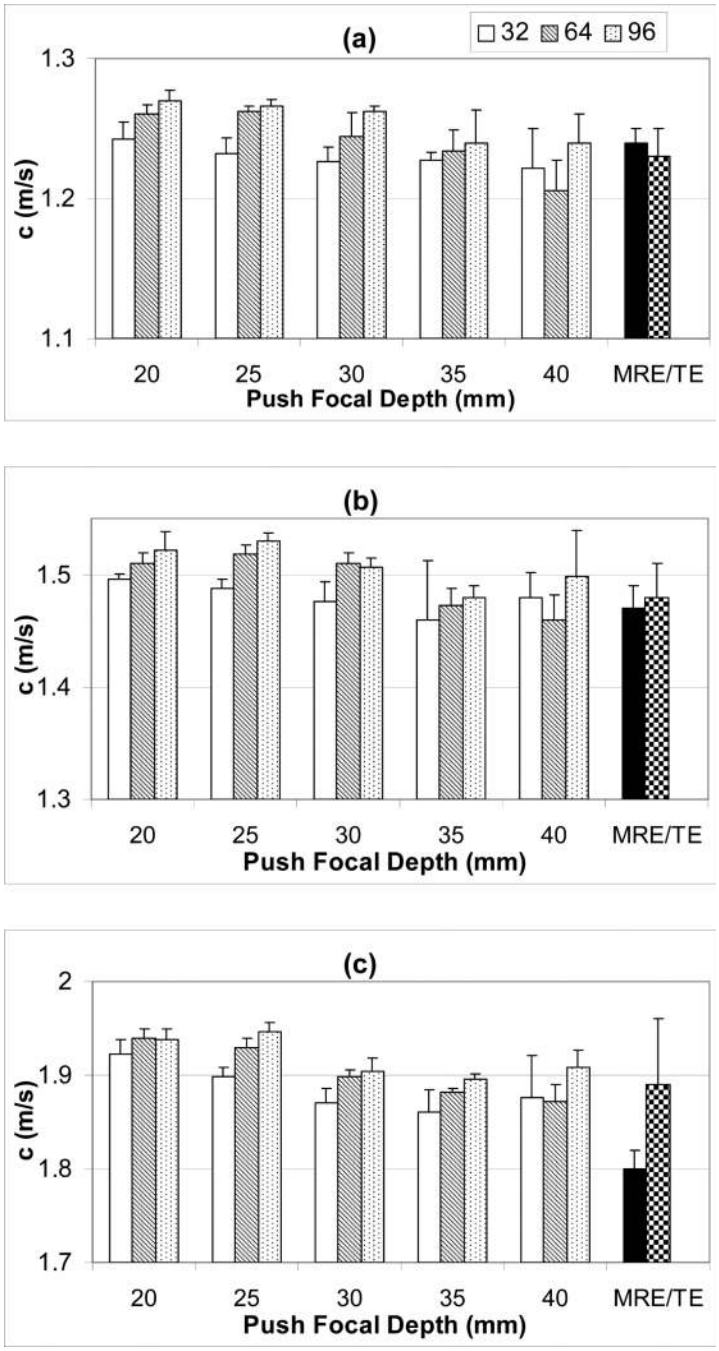

Fig. 3.

Shear wave speeds measured by L7-4 (elevational focus: 25 mm) in phantom 1 (a), phantom 2 (b), and phantom 3 (c). At each measurement depth, 3 different aperture sizes (32, 64, and 96 elements) were used for push beam transmission. Results from MRE and 1D TE are also displayed for comparison.

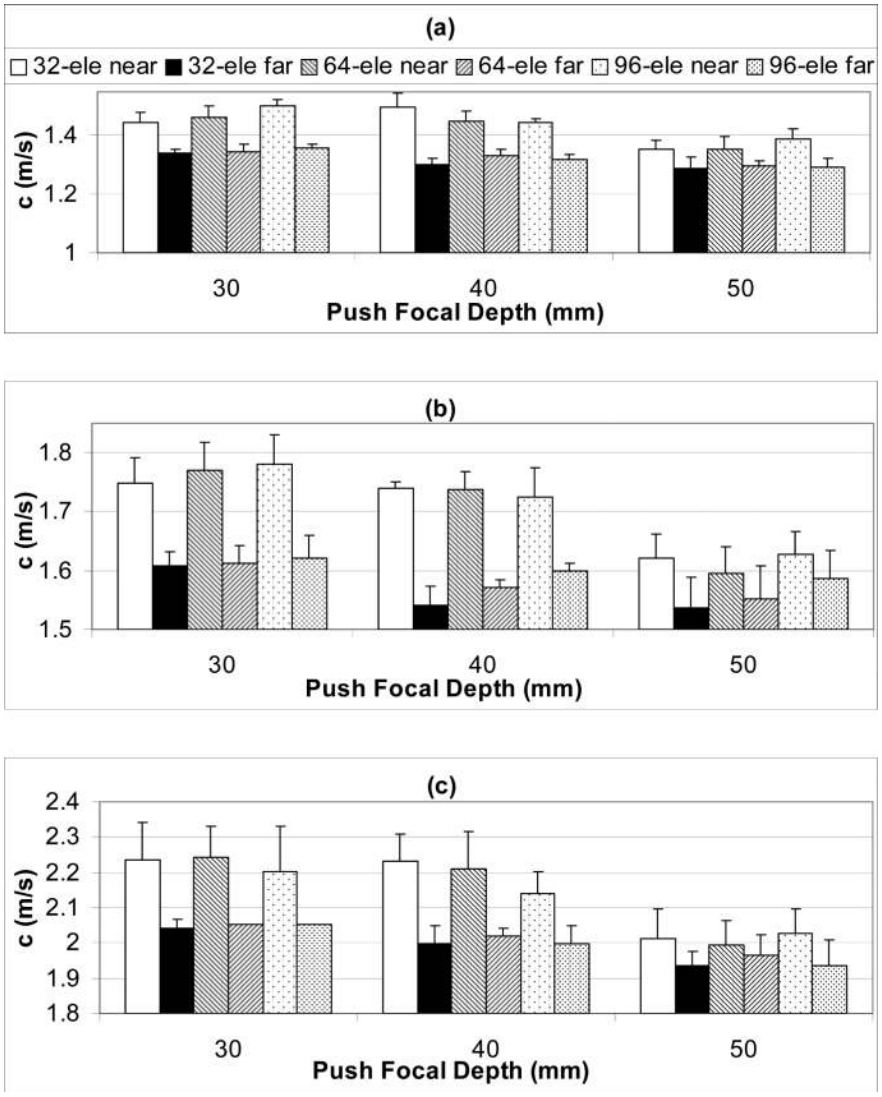

Fig. 4.

Shear wave speed measured by C4-2 using two different lateral ranges (near: 0~7.7 mm, far: 7.7~15.4 mm) from the push beam in phantom 1 (a), phantom 2 (b), and phantom 3 (c). At each measurement depth, 3 different aperture sizes (32, 64, and 96 elements) were used for push beam transmission.

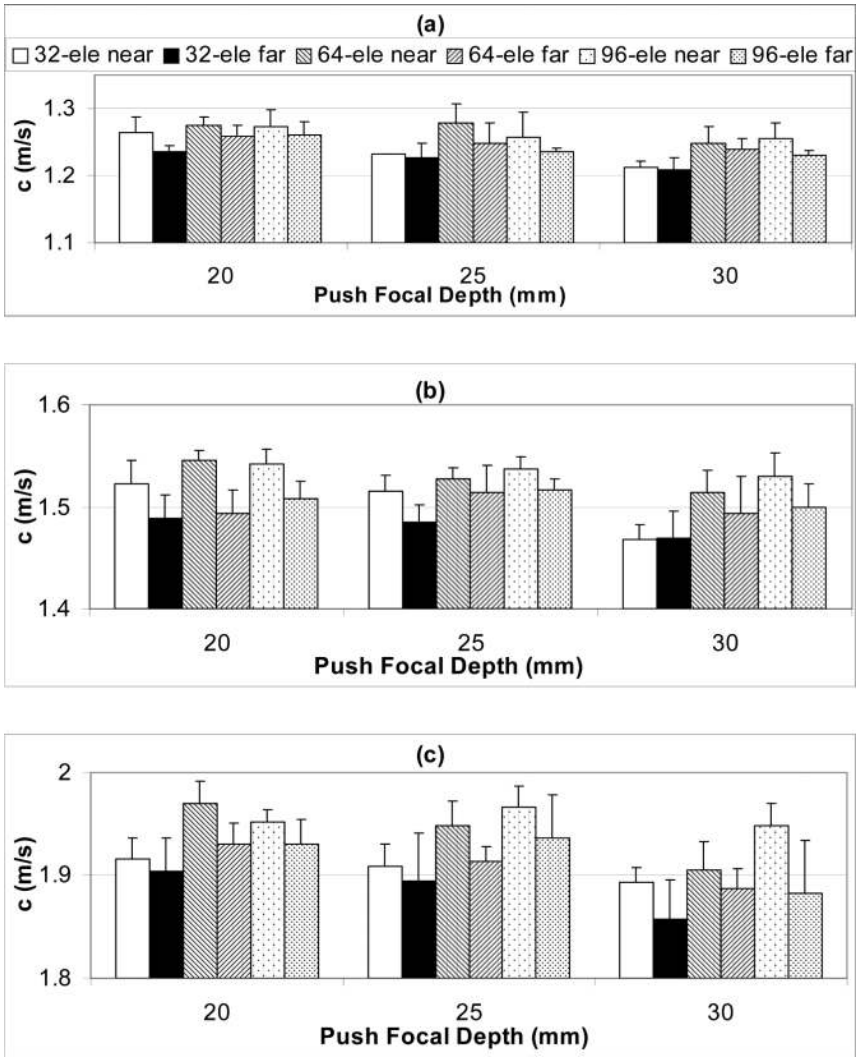

Fig. 5.

Shear wave speed measured by L7-4 using two different lateral ranges (near: 0~9.24 mm, far: 9.24~18.48 mm) from the push beam in phantom 1 (a), phantom 2 (b), and phantom 3 (c). At each measurement depth, 3 different aperture sizes (32, 64, and 96 elements) were used for push beam transmission.

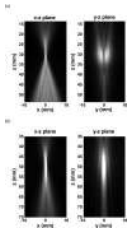

Fig. 6.
Normalized intensity field of the C4-2 measured experimentally in the midelevational plane (*x*-*z* plane) and mid-lateral plane (y-z plane) when the transducer was focused at 30 mm (a) or 50 mm (b).

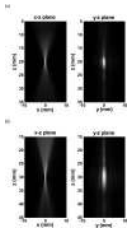

Fig. 7.
Normalized intensity field of the L7-4 measured experimentally in the mid-elevational plane (*x*-*z* plane) and mid-lateral plane (*y*-*z* plane) when the transducer was focused at 20 mm (a) or 30 mm (b).

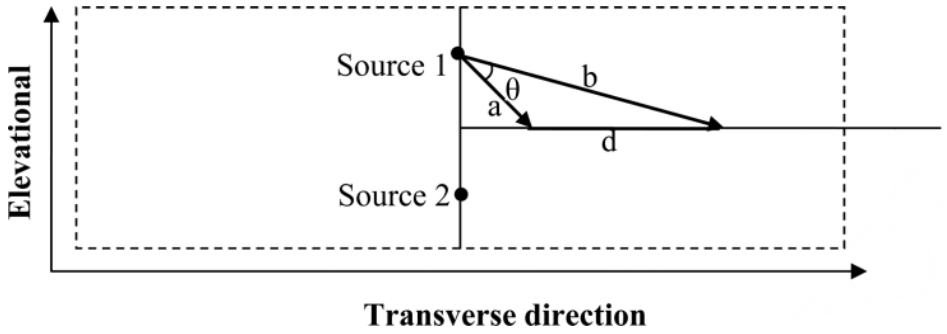

Fig. 8.
Schematic plot of bias caused by shear wave propagating from the split peaks in elevational direction.

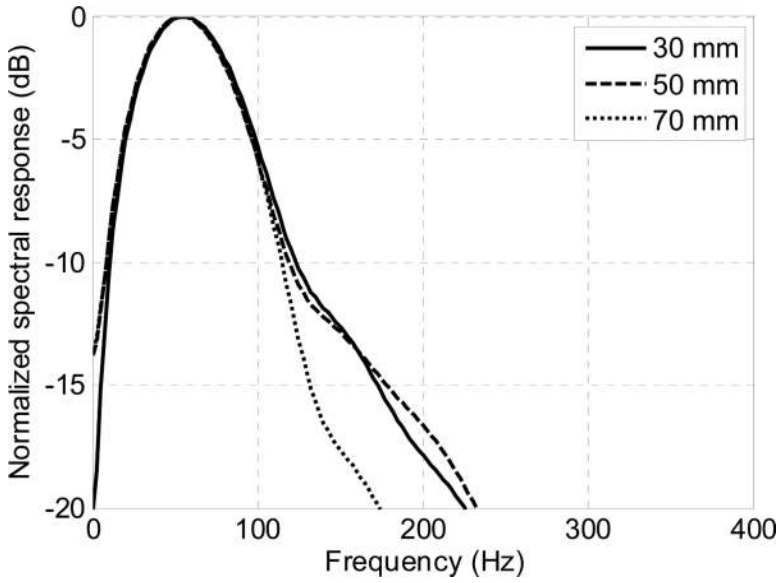

Fig. 9.
Power spectra of shear waves (recorded 5 mm away from the push beam) generated by the C4-2 with different focal depths in phantom 1.

Table 1

Phantom shear wave speeds measured by MRE and 1D TE (m/s)

	MRE	1D TE
Phantom 1	1.24 ± 0.01	1.23±0.02
Phantom 2	1.47 ± 0.02	1.48±0.03
Phantom 3	1.80 ± 0.02	1.89±0.07

Table 2

p-values of paired t-test for depth (non-significant values are shown in bold).

	25 mm	**30 mm**	**35 mm**	**40 mm**
20 mm	**0.3861**	<0.01	<0.01	<0.01
25 mm		<0.01	<0.01	<0.01
30 mm			<0.01	**0.0577**
35 mm				**0.8292**